A kinetic study on the catalysis of KCl, K₂SO₄, and K₂CO₃ during oxy-biomass combustion

Shuanghui Deng [a], Xuebin Wang [a, *], Jiaye Zhang [a], Zihan Liu[a], Hrvoje Mikulčić [b],

Milan Vujanović [b], Houzhang Tan [a], Neven Duić [b]

[a] MOE Key Laboratory of Thermo-Fluid Science and Engineering, Xi'an Jiaotong University,

Xi'an 710049, Shaanxi, China

[b] Faculty of Mechanical Engineering and Naval Architecture, University of Zagreb, Zagreb 10000, Croatia

E-mail: wxb005@mail.xjtu.edu.cn

ABSTRACT

Biomass combustion under the oxy-fuel conditions (Oxy-biomass combustion) is one of the approaches achieving negative CO_2 emissions. KCl, K_2CO_3 and K_2SO_4, as the major potassium species in biomass ash, can catalytically affect biomass combustion. In this paper, the catalysis of the representative potassium salts on oxy-biomass combustion was studied using a thermogravimetric analyser (TGA). Effects of potassium salt types (KCl, K_2CO_3 and K_2SO_4), loading concentrations (0, 1, 3, 5, 8 wt.%), replacing N_2 by CO_2, and O_2 concentrations (5, 20, 30 vol.%) on the catalysis degree were discussed. The comparison between TG-DTG curves of biomass combustion before and after water washing in both the 20%O_2/80%N_2 and 20%O_2/80%CO_2 atmospheres indicates that the water-soluble minerals in biomass play a role in promoting the devolatilization and accelerating the char-oxidation; and the replacement of N_2 by CO_2 inhibits the devolatilization and char-oxidation processes during oxy-biomass combustion. In the devolatilization stage, the catalysis degree of potassium monotonously increases with the increase of potassium salt loaded concentration. The catalysis degree order of the studied potassium salts is $K_2CO_3 > KCl > K_2SO_4$. In the char-oxidation stage, with the increase of loading concentration the three kinds of potassium salts present inconsistent change tendencies of the catalysis degree. In the studied loading concentrations from 0 to 8 wt.%, there is an optimal loading concentration for KCl and K_2CO_3, at 3 wt.% and 5 wt.%, respectively; while for K_2SO_4, the catalysis degree on char-oxidation monotonically increases with

the loading potassium concentration. For most studied conditions, regardless of the potassium salt types or the loading concentrations or the combustion stages, the catalysis degree in the O_2/CO_2 atmosphere is stronger than that in the O_2/N_2 atmosphere. The catalysis degree is also affected by the O_2 concentrations, and the lowest catalysis degree is generally around 20 vol.% O_2 concentration. The kinetic parameters under the different studied conditions are finally obtained.

Keywords: Biomass; Oxy-fuel combustion; Catalysis; Potassium; Thermogravimetric analysis.

1. Introduction

The awareness of the increase in greenhouse gas emission has resulted in the use of renewable energy and the development of new technologies that can accommodate capture and sequestration of carbon dioxide (Buhre et al., 2005; Ma et al., 2016). Biomass is considered as the CO_2-neutral fuel because it consumes the same amount of CO_2 during combustion as is absorbed during growth through photosynthesis. In recent decades biomass is not only attracting interest to meet our growing energy demands but facilitating our carbon reduction and renewable energy targets (Demirbas et al., 2009; Wang et al., 2013). Oxy-fuel combustion is a promising carbon capture technology for newly built and retrofitted coal-fired power plants based on the advantages of a relatively moderate efficiency penalty and the lowest retrofit capital expenditure (Chen et al., 2012; Li and Wei, 2013). Therefore, a combining technology which burns biomass under oxy-fuel combustion conditions, named "oxy-biomass combustion", can achieve "CO_2 negative emission" (Wang et al., 2014; Wang et al., 2015a).

There are a significant number of publications relating to alkali metal catalysts, especially potassium salts. However, the mechanisms of alkali metal catalysts are different in different research conditions. Among all the inorganic elements existed in biomass, potassium has the largest effect on catalyzing both biomass pyrolysis and gasification/combustion process as well as its thermal conversion characteristics. Several explanations for the catalytic role played by potassium have been proposed: (1) potassium can decrease the primary tar yield from decomposition and

increase the gas and char products (Jensen et al., 1998; Jones et al., 2007); (2) potassium can enhance the soot oxidation by consuming the carbon to form carbonate species during soot combustion (Querini et al., 1999); (3) potassium can result in the lowest oxidation temperature, increase reaction rates of char combustion and bring higher conversion efficiencies (An and McGinn, 2006; Jones et al., 2007). Further, the potassium in the char is a good catalyst bringing higher conversion efficiencies in terms of carbon burn-out during char combustion process (Nowakowski et al., 2007). However, the high potassium content in biomass induces severe fouling and slagging in biomass-fired furnace (Wang et al., 2012; Ren and Li, 2015). One of the approaches to solve these problems in biomass combustion is to lower the potassium and chlorine contents in the biomass feedstocks (Wang et al., 2011). Water-leaching has proven highly effective at removing the minerals in agriculture biomass (Wang et al., 2015b). Deng et al. (2013) investigated the effect of water washing on biomass properties, and found that water washing removed 80-90 wt.% potassium and relieved ash melting and fouling. However, the water washing also significantly affects the ignition and burnout characteristics of biomass, which indicates the catalysis of potassium on biomass combustion. In air atmosphere, although the catalysis of alkali and alkaline earth metals (AAEMs) on coal combustion and gasification have been widely reported (Backreedy et al., 2003; Nzihou et al., 2013; Quyn et al., 2002; Wagner and Mühlen, 1989), researches on the effect of the potassium catalysis on biomass combustion, especially in an O_2/CO_2 atmosphere, are few.

The concept of oxy-fuel combustion is to remove the nitrogen from air and then to utilize flue gas recycle (mainly carbon dioxide and moisture) to proceed the combustion process in oxygen (Toftegaard et al., 2010). Based on the aspects of combustion chemistry, mass transfer and radiation heat transfer, the coal combustion process in oxy-combustion is expected different with that in traditional air combustion. CO_2 has a larger specific molar heat than N_2, and coal may be gasified by the CO_2, thus the use of CO_2 instead of N_2 causes a reduction in the particle surface temperature, flame propagation speed and stability of the flame as well as an increase in the unburned carbon content. These problems can be overcame by increasing an oxygen concentration in oxy-fuel combustion (Gil et al., 2012;

Bejarano and Levendis, 2008; Zhou et al., 2016). In the past decade, quite a lot of investigations have been made to probe into different challenges associated with the ignition and burnout during oxy-fuel combustion. Under oxy-fuel combustion conditions, the combustion environment is significantly changed in oxygen concentration and temperature, depending on the combustion method types, thereby, the catalytic effects of AAEMs on the devolatilization and char-oxidation might be also affected. However, these catalytic effects of AAEMs on biomass combustion process in oxy-fuel combustion environment have not been reported in the present literatures.

This paper aims to investigate the catalysis effects of potassium on the devolatilization and the char-oxidation stages under air and oxy-biomass combustion conditions, and to seek if its catalytic influences are meaningful in these conditions. The effects of potassium salt types (KCl, K_2CO_3, and K_2SO_4), loading concentrations (0, 1, 3, 5, 8 wt.%), replacing N_2 by CO_2, and O_2 volume concentrations (5, 20, 30 vol.%) on the catalysis degree are studied in a thermogravimetric analysis (TGA) reactor.

2. Materials and methods

2.1. Material samples

The biomass used in this study is the wheat straw from Baoji district of Shaanxi province, China. Table 1 shows the proximate and ultimate analysis of raw wheat straw sample. The straw particles were pulverized and sieved into ≤ 200 μm.

Table 1 The proximate and ultimate analyses of raw straw sample.

M_{ad} (wt.%)	C_{ad} (wt.%)	H_{ad} (wt.%)	N_{ad} (wt.%)	O_{ad} (wt.%)	S_{ad} (wt.%)	$Q_{gr,d}$ (kJ/kg)
3.25	41.31	5.78	1.21	50.98	0.72	18.83

To remove the minerals from the straw sample, the procedures of a hot water wash were applied. In the hot water wash, 10 g of straw were stirred in a beaker with 200 ml of deionized water at 80 °C for 6 h. After that, the water washed straw was filtrated, washed with 200 ml of deionized water and then dried in an oven at 80 °C for 24 h. Table 2 shows the ash composition analysis of both raw and water washed straw samples. From Table 2, after water washing,

the content of potassium and sulfur in the ash decreased from 13.5 % to 3.1%, and from 2.6% to 0.8%, respectively, and

no chlorine was detected. Since the ash content was lowered by about half, the removing rates of K, Cl and S by water

washing were 88.5, 100 and 84.6%, respectively.

Table 2 Composition analysis of raw straw ash and water washed straw ash

Samples	Ash chemical compositions (wt. %)									
	K	Cl	S	Ca	Mg	P	Fe	Si	Al	O
Raw straw	13.5	2.0	2.6	15.0	5.2	1.9	3.1	15.8	2.3	38.7
Water washed straw	3.1	0.0	0.8	13.1	3.80	1.4	4.5	27.1	3.2	43.0

In order to add potassium to the water washed straw sample, the three kinds of potassium salts including KCl,

K_2CO_3 and K_2SO_4 were impregnated, respectively. For each kind of potassium salt, 0.005 g of potassium salt and 3 ml

of deionized water were added into 0.495 g of the water washed straw in a glass beaker. The solution was thoroughly

mixed for 12 h by a stirrer to make a distribution of the potassium salt uniform. After that, the mixed solution was dried

for 24 h in an 80 °C oven. Thus, 1 wt% loading concentration of potassium salts including KCl, K_2CO_3 and K_2SO_4 in

the water washed straw samples were obtained, respectively. In the resemble operation conditions, 3, 5 and 8 wt%

potassium salts including KCl, K_2CO_3 and K_2SO_4 were impregnated, respectively. In this paper, the raw straw sample

and the water washed straw sample are labeled as R_o and A_o, respectively. The serial numbers of samples with different

loading potassium salt types (KCl, K_2CO_3 and K_2SO_4) and loading concentrations (1, 3, 5, 8 wt.%) are shown in Table

3.

Table 3 The sample numbers of different loading concentrations and potassium salt types.

Sample Nos.	Loading concentrations	Sample Nos.	Loading concentrations
K_{A1}	1 wt.% KCl	K_{B5}	5 wt.% K_2CO_3
K_{A3}	3 wt.% KCl	K_{B8}	8 wt.% K_2CO_3
K_{A5}	5 wt.% KCl	K_{C1}	1 wt.% K_2SO_4
K_{A8}	8 wt.% KCl	K_{C3}	3 wt.% K_2SO_4
K_{B1}	1 wt.% K_2CO_3	K_{C5}	5 wt.% K_2SO_4
K_{B3}	3 wt.% K_2CO_3	K_{C8}	8 wt.% K_2SO_4

2.2. Thermogravimetric analysis methods

Thermogravimetric analysis was performed in a STA-409PC thermal analyzer (NETZSCH, German). 5±0.1 mg of

samples were loaded into an Al_2O_3 crucible for each run. In the experiments, the samples were carried out over a temperature range of 30-750 °C at a heating rate of 20 °C/min. The O_2 volume concentrations in the total carrier gas (O_2/N_2 or O_2/CO_2) flow of 100 ml/min were 5, 20 and 30 vol.%, respectively. In TG and DTG curves, T_i is the ignition temperature (biomass volatile), °C; T_f is the burnout temperature (biomass char), °C; T_{peak1} is the temperature of the first peak in DTG curves (volatile release), °C; w_{max1} is the peak value of the first peak in DTG curves (volatile release), %/min; T_{peak2} is the temperature of the second peak in DTG curves (char-oxidation), °C; w_{max2} is the peak value of the second peak in DTG curves (char-oxidation), %/min.

3. Results and discussion

3.1. Effects of water washing and atmosphere on the biomass combustion

For the convenience of comparison under the varied conditions, T_i, T_f, T_{peak1}, w_{max1}, T_{peak2}, and w_{max2} of straw combustion under all the conditions are summarized in Table 4.

Table 4 Characteristic parameters on TG-DTG curves of straw combustion for all the studied conditions.

Atmosphere	O_2	No.	T_i/°C	T_f/°C	T_{peak1}/°C	w_{max1}/ wt.%·min^{-1}	T_{peak2}/°C	w_{max2}/ wt.%·min^{-1}
O_2/N_2	5%	A_0	299.8	504.7	350.7	21.63	477.1	4.26
O_2/N_2	5%	K_{C5}	283.3	470.9	340.3	16.85	427.5	6.72
O_2/N_2	20%	R_0	265	453.8	302.8	19.45	442.3	14.83
O_2/N_2	20%	A_0	281.9	471.9	330.9	20.71	441.8	6.09
O_2/N_2	20%	K_{C1}	286	467.8	333.3	21.61	433.4	5.73
O_2/N_2	20%	K_{C3}	281.9	459.2	330.8	20.06	416.3	6.79
O_2/N_2	20%	K_{C5}	283.2	447.5	330	20.74	405.5	11.86
O_2/N_2	20%	K_{C8}	280.8	445.1	330.3	18.73	405.9	10.74
O_2/N_2	20%	K_{B1}	280.4	454.2	326.4	19.58	431.7	7.38
O_2/N_2	20%	K_{B3}	268.4	422.8	302.3	20.98	407.4	14.81
O_2/N_2	20%	K_{B5}	260	446.2	295.5	18.62	437.7	10.61
O_2/N_2	20%	K_{B8}	257.2	483.6	292.8	18.58	436.1	6.02
O_2/N_2	20%	K_{A1}	281.2	463.1	330	20.14	438	6.47
O_2/N_2	20%	K_{A3}	273.9	454.7	315.7	20.99	441.8	6.38
O_2/N_2	20%	K_{A5}	272.8	448.7	311.9	23.04	433.7	7.66
O_2/N_2	20%	K_{A8}	271.4	450.8	313	20.94	439.5	9.11
O_2/N_2	30%	A_0	292.4	470.6	331.9	27.22	440.2	5.75

O_2/N_2	30%	K_{C5}	281.1	425	324.5	22.81	395.2	17.95
O_2/CO_2	5%	A_0	306.6	513.9	354.9	21.83	467.5	3.67
O_2/CO_2	5%	K_{C5}	284.4	485.9	344.2	15.91	442.1	5.74
O_2/CO_2	20%	R_0	266.1	481.3	304.7	18.47	471.2	8.95
O_2/CO_2	20%	A_0	306.9	500	342.9	23.38	456.5	4.72
O_2/CO_2	20%	K_{C1}	290.3	474.5	337	20.56	440.6	5.24
O_2/CO_2	20%	K_{C3}	282.3	465.7	333	18.95	422.6	5.82
O_2/CO_2	20%	K_{C5}	283.7	448.6	332.6	19.23	416.4	8.26
O_2/CO_2	20%	K_{C8}	281.6	440	330.5	18.25	408.1	9.16
O_2/CO_2	20%	K_{B1}	283.1	470.2	331.2	17.95	441	5.44
O_2/CO_2	20%	K_{B3}	272.3	453.8	304.3	19.86	410.9	6.47
O_2/CO_2	20%	K_{B5}	262.2	474.2	297	18.45	453.8	5.23
O_2/CO_2	20%	K_{B8}	257.2	484.9	294.9	16.56	461.4	6.31
O_2/CO_2	20%	K_{A1}	280.8	474.2	332.6	18.54	444.9	4.92
O_2/CO_2	20%	K_{A3}	275.9	468.4	318.7	20.14	415.6	5.08
O_2/CO_2	20%	K_{A5}	274.1	473.8	318.5	19.15	411.2	4.93
O_2/CO_2	20%	K_{A8}	272.8	471.3	315.3	19.36	458.7	4.88
O_2/CO_2	30%	A_0	302.3	477.8	337.8	29.24	439.7	5.38
O_2/CO_2	30%	K_{C5}	260.4	448.1	291.9	20.67	452.6	4.57

TG-DTG curves of straw combustion before and after water washing, in both $20\%O_2/80\%N_2$ and $20\%O_2/80\%CO_2$ atmospheres, are compared in Fig. 1. Compared with raw straw, both the first DTG peak (devolatilization) and the second DTG peak (char-oxidation) of A_0 is delayed after water washing. In addition, the peak height of A_0 becomes much lower and wider. In DTG curves, the peak height represents the burning rate, indicating that the removal of water-soluble minerals leads to a significant inhibition on char-oxidation rate. Comparing the differences of TG-DTG curves with respect to R_0 and A_0, it is concludes that the water-soluble minerals in biomass play a role in promoting devolatilization and accelerating char-oxidation during biomass combustion process.

In addition, the comparison between $20\%O_2/80\%N_2$ (solid lines) and $20\%O_2/80\%CO_2$ (dashed lines) atmospheres shows that the change of balanced gas from N_2 to CO_2 results in a delay on both devolatilization and char-oxidation peaks. From Fig. 1, for raw straw combustion, the temperature ranges of the devolatilization stage are at around 190-410 °C in $20\%O_2/80\%N_2$ atmosphere and at around 200-440 °C in $20\%O_2/80\%CO_2$ atmosphere, respectively;

while the ones of the char-oxidation stage are at around 410-540 °C in 20%O_2/80%N_2 atmosphere and at around

440-550 °C in 20%O_2/80%CO_2 atmosphere, respectively. However, for water washed straw combustion, the

temperature ranges of the devolatilization stage are at around 195-390 °C in 20%O_2/80%N_2 atmosphere and at around

210-400 °C in 20%O_2/80%CO_2 atmosphere, respectively; while the ones of the char-oxidation stage are at around

390-550 °C in 20%O_2/80%N_2 atmosphere and at around 400-560 °C in 20%O_2/80%CO_2 atmosphere, respectively. It is

concluded that the replacement of N_2 by CO_2 inhibits both the devolatilization and the char-oxidation stages during

oxy-biomass combustion. This inhibition is explained from three aspects: (1) the relative diffusivity of O_2 in CO_2

atmosphere is lower than that in N_2 atmosphere; (2) the specific heat capacity of CO_2 is larger than N_2 and much higher

concentration enhances the endothermic reaction of gasification between char and CO_2 (Zhou et al., 2016); (3) In the

20%O_2/80%CO_2 atmosphere, for the char-oxidation stage, the much higher CO_2 concentration hindered the exothermic

reaction $C + O_2 \rightleftharpoons CO_2$ to forward direction, resulting in a lower char particle temperature than that in the

20%O_2/80%N_2 atmosphere. These three reasons lead to the decrease in particle temperature.
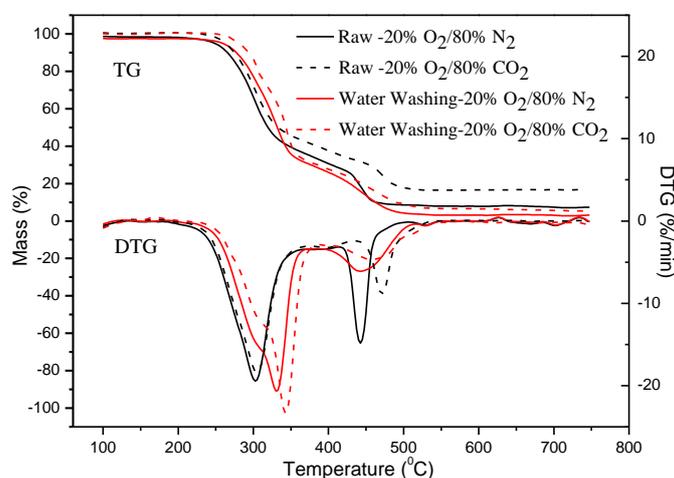
Fig. 1. The effects of water washing and atmosphere on TG-DTG curves of oxy-biomass combustion.

3.2. Effects of potassium salt type and concentration on the catalytic oxy-biomass combustion

The TG-DTG curves of straw combustion with different potassium salt types (KCl, K_2CO_3 and K_2SO_4) and

loading concentrations (0, 1, 3, 5, 8 wt.%) under both O_2/CO_2 and O_2/N_2 atmospheres are presented in Fig.2. The

characteristic temperatures under different conditions are summarized and compared in Fig. 3. In this part, we focus on

the discussion on the effects of potassium types and loading concentrations on the catalysis degree, and the effects of atmosphere will be discussed in the 3.3 section. From Fig. 2 and 3, after loading potassium salt, the general decreases of these four characteristic temperatures (T_i, T_{peak1}, T_{peak2}, and T_f) are observed, in which T_i and T_{peak1} reflect the devolatilization stage while T_{peak2} and T_f reflect the char-oxidation stage. For the devolatilization stage, the two characteristic temperatures of T_i and T_{peak1} monotonically decrease with the increase of potassium salt loaded concentration. The most drastic decreases of T_i and T_{peak1} happen when the loading concentration increases from 1 to 3 wt.%; and when the loading concentration is beyond 5 wt.%, the increase becomes slow. Among the three potassium salts, K_2CO_3 has the best catalytic ability, because its devolatilization peak temperature decreases by 60 °C at a loading concentration of 8 wt.% under oxy-biomass combustion conditions. By comparison, the decrease values by the 8 wt.% loading of K_2SO_4 and KCl are 25 °C and 40 °C, respectively. It can be seen that the catalysis degree order of the studied potassium salts is $K_2CO_3 > KCl > K_2SO_4$. Moreover, the catalytic degree in O_2/CO_2 atmosphere is stronger than that in O_2/N_2 atmosphere, e.g., the change of devolatilization temperatures with K_2SO_4 loaded in O_2/N_2 atmosphere is negligible.
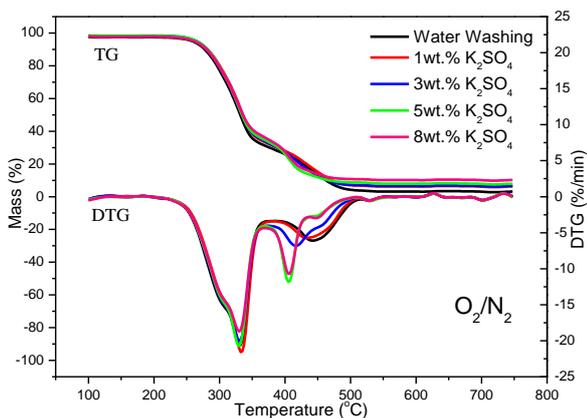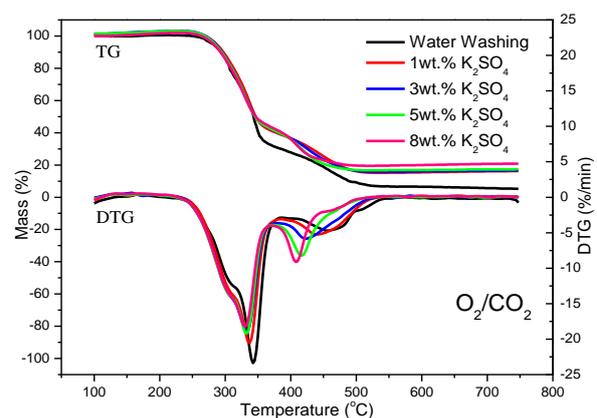
(a)   (b)
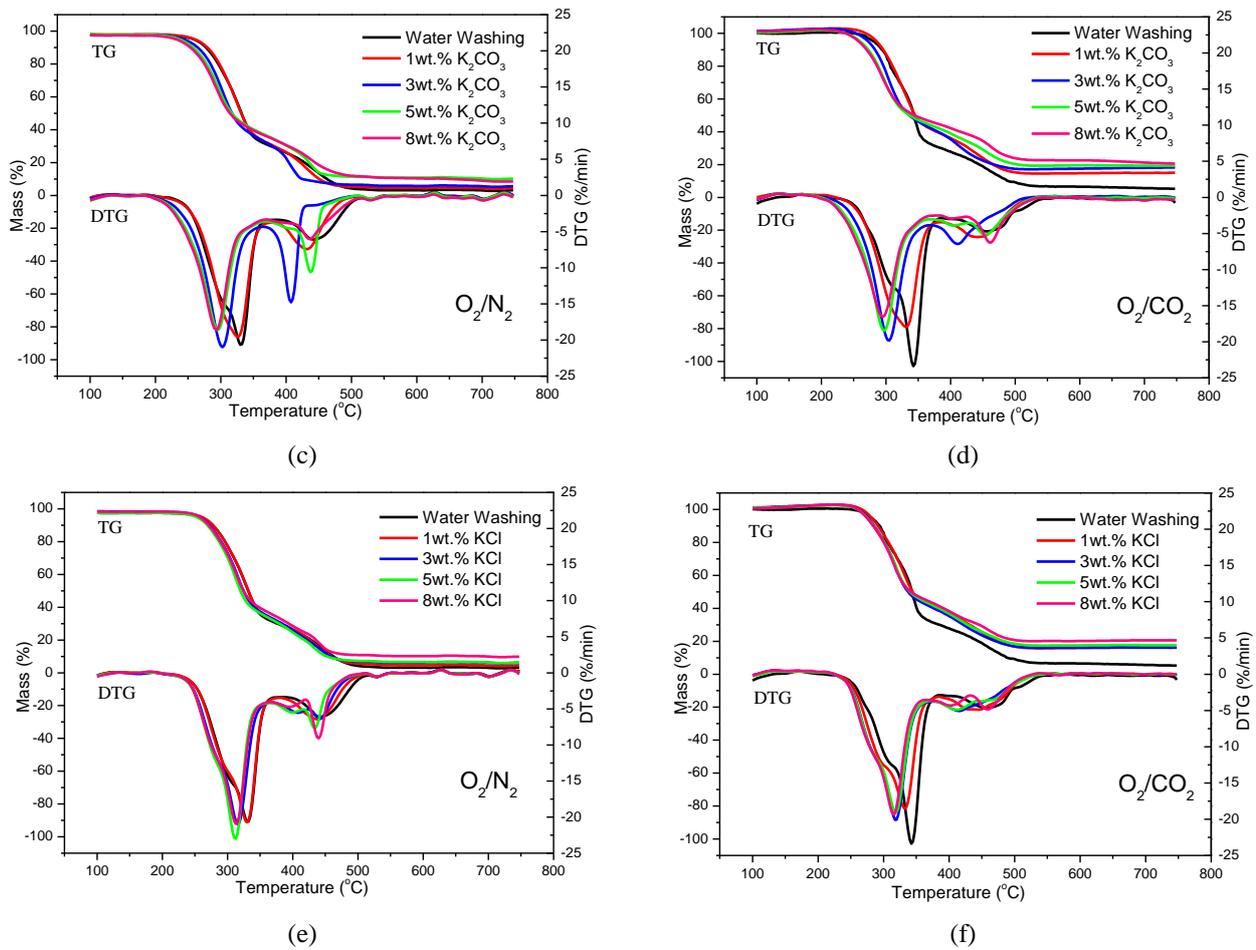
Fig. 2. TG-DTG curves of straw combustion with different potassium types and loading concentrations. a-K_2SO_4, O_2/N_2; b-K_2SO_4, O_2/CO_2; c-K_2CO_3, O_2/N_2; d-K_2CO_3, O_2/CO_2; e-KCl, O_2/N_2; f- KCl, O_2/CO_2.

For the char-oxidation stage, with the increase of loading concentration, the three kinds of potassium salts present inconsistent overall change tendencies of the characteristic temperatures (T_{peak2} and T_f). There is an optimal loading concentration for the lowest peak temperatures of char-oxidation for KCl and K_2CO_3 loaded samples, at 3 wt.% and 5 wt.%, respectively; while for K_2SO_4 loaded samples, with the increase of loading concentration, the characteristic temperatures of char-oxidation monotonically decrease. Depending on the loading concentration and the atmosphere, all studied potassium slats have the abilities to decrease the char-oxidation peak temperature by 40-45 °C. By comparing O_2/N_2 and O_2/CO_2 atmospheres, it is observed that there is a huge different changing tendency for K_2CO_3 catalysis. The catalysis of KCl on the char-oxidation in O_2/N_2 atmosphere is marginal, while in O_2/CO_2 atmosphere it reaches the best at the loading concentration of 5 wt.%, generating a decrease of peak temperature by 45 °C.

As the increase of the loading concentration during biomass combustion in TGA reactor, the different changing tendencies indicate the different catalysis mechanisms of potassium in both the devolatilization stage and the char-oxidation stage. It is noted that in TGA reactor, the temperature range of the first stage of devolatilization is below 400 °C, which is insufficient for a real ignition of volatile component. The mass loss in the first stage is mainly due to the devolatilization process. Therefore, in the first stage the catalysis of potassium salts takes its influence by accelerating the devolatilization process (Jones et al., 2007).

However, the catalytic acceleration mechanisms with metal loaded for biomass char-oxidation have been classified as "electron-transfer theories" or "oxygen-transfer theories", while more and more recent studies believe the latter can give a better explanation, especially in combustion process with adequate oxygen. In "oxygen-transfer theories", it has been suggested that alkali metal atoms on carbon surface act as the active sites for the chemisorption of oxygen, thereby weakening C=C surface bonds and promoting the desorption of the CO and CO_2 products (Wagner and Mühlen, 1989; Shen and Qin, 2006; Wang et al., 2017). This result has been proven by the temperature-programmed desorption test (Freriks et al., 1981; Cerfontain and Moulijn, 1983; McKee, 1983).
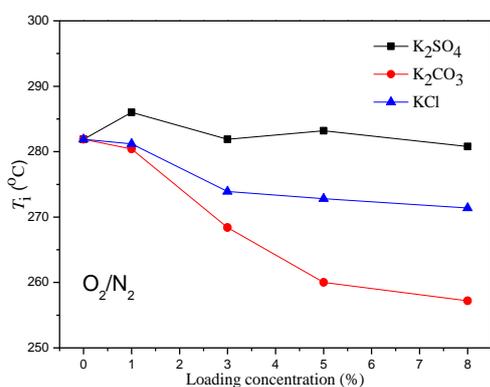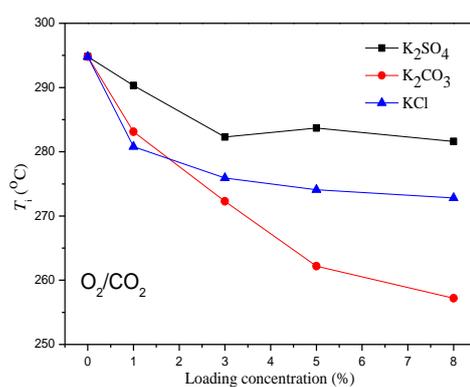
(a)   (b)
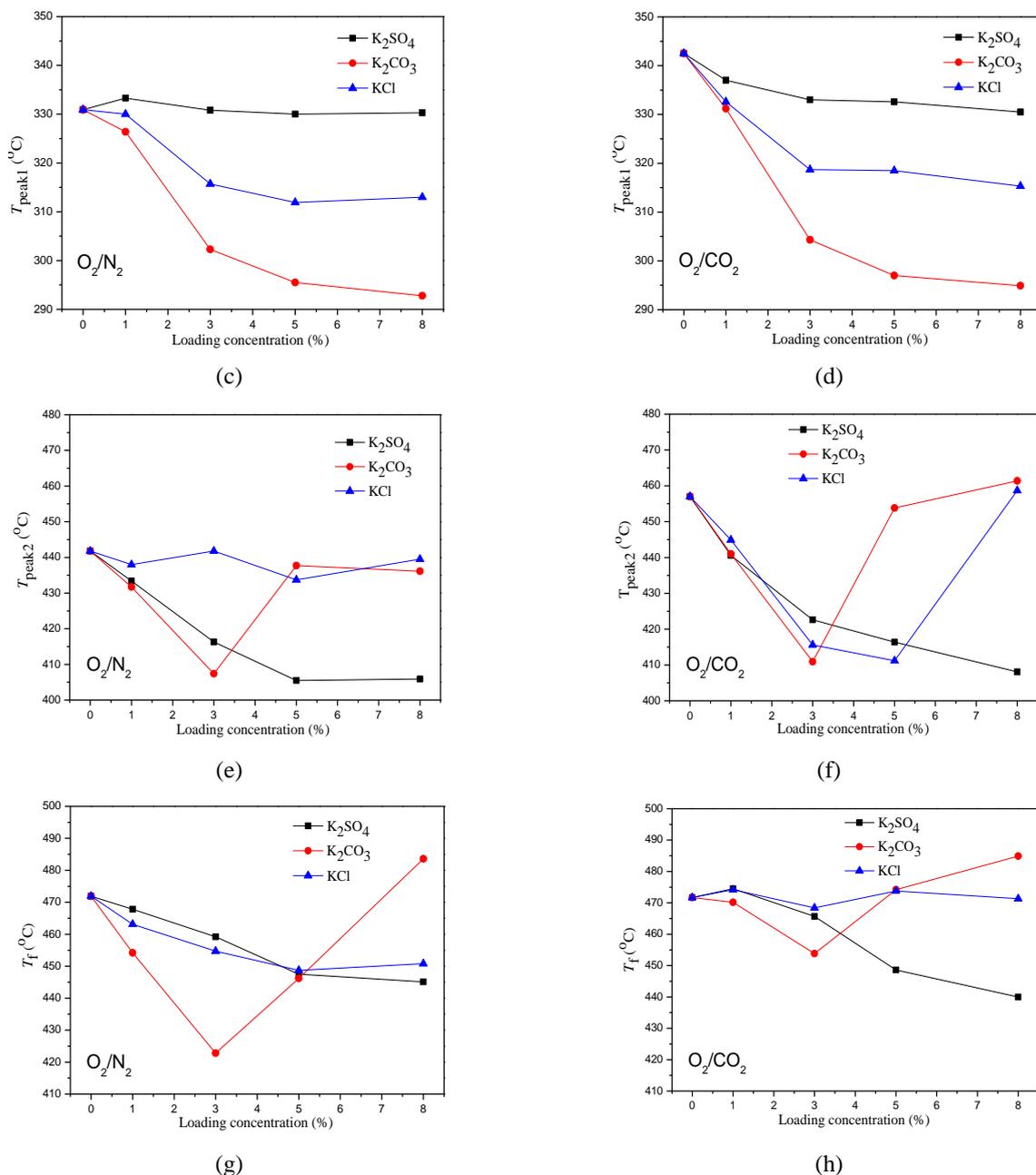
Fig. 3. Characteristic temperatures of straw combustion with different loading potassium types and concentrations. a-T_i, O_2/N_2; b-T_i, O_2/CO_2; c-T_{peak1}, O_2/N_2; d-T_{peak1}, O_2/CO_2; e-T_{peak2}, O_2/N_2; f-T_{peak2}, O_2/CO_2; g-T_f, O_2/N_2; h-T_f, O_2/CO_2.

3.3. Effects of atmospheres on the catalysis of potassium during oxy-biomass combustion

3.3.1. Comparison of the potassium catalysis in the O_2/N_2 and O_2/CO_2 atmospheres

In order to more clearly compare the potassium catalysis in the O_2/N_2 and O_2/CO_2 atmospheres, we replot the differences of the peak temperatures (ΔT_{peak1} and ΔT_{peak2}) before and after loading potassium as the criterion of catalysis degree, as shown in Fig. 4. For most studied conditions, regardless of the potassium salt types or the loading concentrations, the O_2/CO_2 atmosphere produces a larger decrease of the peak temperatures for both the devolatilization

12

and char-oxidation stages compared with the O_2/N_2 atmosphere. This indicates that the potassium in O_2/CO_2 atmosphere exerts a more significant catalytic effect than that in O_2/N_2 atmosphere.

(a)   (b)
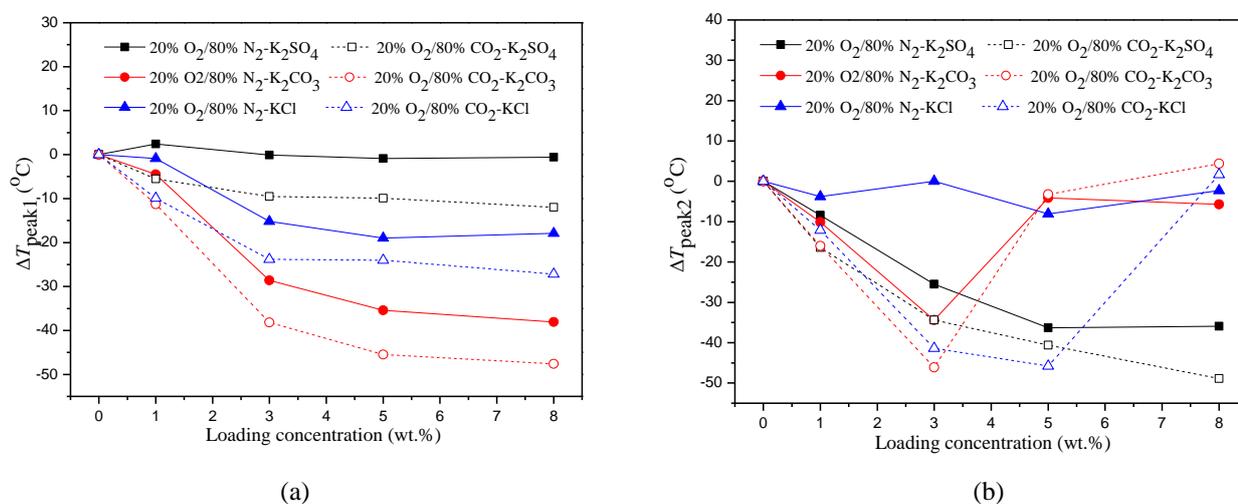
Fig. 4. The comparison of catalysis degree between O_2/N_2 and O_2/CO_2 atmospheres. a-ΔT_{peak1}; b-ΔT_{peak2}.

3.3.2. The effects of O_2 concentrations

The effects of O_2 concentrations (5, 20, and 30 vol.%) in different atmospheres on the catalytic oxy-biomass combustion in TGA reactor are studied under the conditions with 5 wt.% K_2SO_4 loaded sample in O_2/CO_2 atmosphere. TG-DTG curves and characteristic parameters under different O_2 atmospheres are summarized in Fig. 5 and 6, respectively. First, for all studied O_2 concentrations, after loading K_2SO_4 both devolatilization and char-oxidation curves move forward to the lower temperatures. On the other hand, the catalysis degree is affected by the O_2 concentrations. The catalysis degree can be expressed by the difference between each pair of curves (solid line for water washed samples and dashed line for 5 wt.% K_2SO_4 loaded samples). It is observed that the lowest catalysis degree (the smallest difference) is generally at 20 vol.% O_2 concentration, which agrees with our previous results on the catalysis of potassium during soot oxidation (Wang et al., 2017).
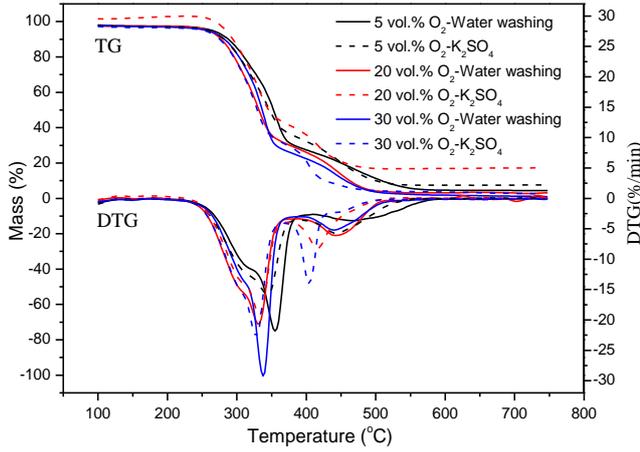
Fig. 5. TG-DTG curves of oxy-biomass combustion at 5, 20, 30 vol.% O_2 concentrations.
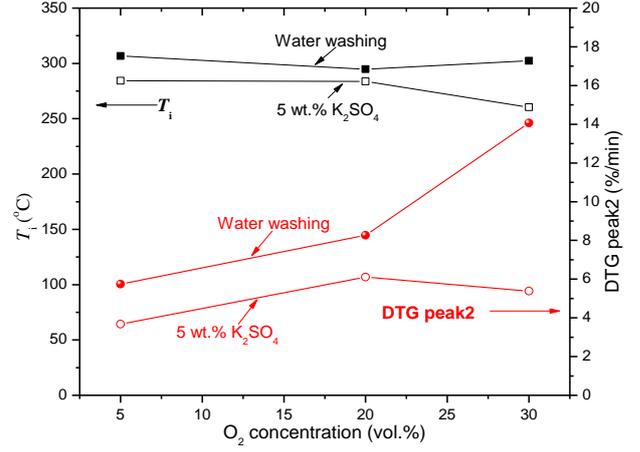
Fig. 6. Effect of O_2 concentration on characteristic parameters of TG-DTG curves.

3.4. Kinetic analysis

The fundamental kinetic equations of biomass combustion reactions can be expressed by Arrhenius equation as follows (Jayaraman and Gökalp, 2015):

$$d\alpha / dt = Kf(\alpha) \tag{1}$$

$$K = Ae^{-E/RT} \tag{2}$$

where K is the reaction rate; α is the conversion degree of combustion material; A is the pre-exponential factor, s^{-1}; E is the activation energy, $kJ \cdot mol^{-1}$; R is the universal gas constant, $8.314 J \cdot mol^{-1} \cdot K^{-1}$; T is the absolute temperature, K; $f(\alpha)$ represents the reaction model function, which is generally described as (Jayaraman and Gökalp, 2015):

$$f(\alpha) = (1-\alpha)^n \tag{3}$$

where n is the order of the reaction.

The above rate expressions can be transformed into non-isothermal rate expressions describing reaction rates as a function of temperature:

$$d\alpha / dt = Ae^{-E/RT}(1-\alpha)^n \tag{4}$$

For a constant heating rate β ($^\circ C \cdot min^{-1}$), $\beta = dT/dt$, Eq. (2) can be transformed into:

$$d\alpha / dT = A\beta^{-1}e^{-E/RT}(1-\alpha)^n \tag{5}$$

14

By integrating, Eq. (5) gives:

$$\int_0^\alpha \frac{d\alpha}{(1-\alpha)^n} = \frac{A}{\beta}\int_{T_0}^T e^{-E/RT}dT \qquad (6)$$

□ The form of f (α) in Eq. (3) depends on the type of reaction model controlling the overall process. The oxygen concentration has a significant effect on the second stage of straw combustion. In the first stage of devolatilization of straw combustion, mainly the pyrolysis stage, most of aliphatic C-O bonds were broken and only part of oxidization of volatiles released and C-H bonds were influenced by oxygen concentration (Fang et al., 2006). In the second stage of char-oxidation, mainly the combustion stage, the C-C bonds were oxidized to C=O and C-O bonds (Fang et al., 2006). So, the oxygen concentration presents more important effects on E in the second stage of straw combustion than that in the first stage. For the chemical control regime in the combustion process, carbon is generally agreed to react with oxygen following a single-step deceleration type function (Sima-Ella and Mays, 2005; Gómez-Barea and Ollero, 2006), in which case f (α) = (1-α) (first-order kinetics with respect to carbon). In addition, the kinetics of pyrolysis and combustion were largely used by a first order reaction model and this model agree well with the TGA experimental data (Jayaraman and Gökalp, 2015; Su et al., 2013; Fang et al., 2006). Thus, n was selected as 1 in the Eq. (6) and a reaction order of n=1 was used to calculate the kinetic parameters in this study.

When n=1, rearranging Eq. (6) and integrating gives:

$$\ln[-\ln\frac{(1-\alpha)}{T^2}] = \ln[\frac{AR}{\beta E}(1-\frac{2RT}{E})] - \frac{E}{RT} \qquad (7)$$

In Eq. (7), $2RT/E \ll 1$(Coats and Redfern, 1964), the term of $\ln[\frac{AR}{\beta E}(1-\frac{2RT}{E})]$ varies linearly with 1/T as slope of the line is –E/R. When $y = \ln[-\ln\frac{(1-\alpha)}{T^2}]$, a=ln(AR/βE) and a is a constant, $b=-E/R$, x=1/T, Eq. (7) can be transformed into：：

$$y=a+bx \qquad (8)$$

In this study, the kinetic parameters can be determined by assuming the reaction orders of devolatilization and

15

char-oxidation as 1. By plotting y vs. x, which corresponds to the two stages, E and A can be obtained as a function of the conversion degree. Kinetic parameters under the different studied conditions are summarized in Table 5.

Table 5 Kinetic parameters of straw combustion for all studied conditions.

Atmospheres	Sample No.	Stages	n	r	A/s^{-1}	E/kJ mol^{-1}
20%O$_2$/80%N$_2$	R$_0$	①	1	-0.98658	1.25E+07	115.51
		②	1	-0.98938	1.33E+01	59.47
	A$_0$	①	1	-0.99589	1.30E+07	117.61
		②	1	-0.97478	1.86E-01	34.88
	K$_{C1}$	①	1	-0.98482	3.53E+08	133.40
		②	1	-0.98946	2.73E-01	36.85
	K$_{C3}$	①	1	-0.98627	7.50E+06	115.68
		②	1	-0.98437	2.93E-01	36.43
	K$_{C5}$	①	1	-0.99109	1.22E+09	138.54
		②	1	-0.98918	1.85E-01	*33.57*
	K$_{C8}$	①	1	-0.98931	5.16E+06	113.79
		②	1	-0.99286	3.28E-01	36.52
	K$_{B1}$	①	1	-0.98925	1.35E+07	118.07
		②	1	-0.97808	1.71E-01	33.96
	K$_{B3}$	①	1	-0.99022	1.41E+05	94.61
		②	1	-0.96849	3.56E-01	36.45
	K$_{B5}$	①	1	-0.98164	1.27E+05	93.33
		②	1	-0.95678	1.01E-01	31.13
	K$_{B8}$	①	1	-0.98599	1.41E+05	93.13
		②	1	-0.98010	1.76E-02	*23.64*
	K$_{A1}$	①	1	-0.99565	8.09E+05	104.66
		②	1	-0.97235	3.00E-01	36.85
	K$_{A3}$	①	1	-0.99160	3.13E+06	109.85
		②	1	-0.98097	2.30E-01	35.21
	K$_{A5}$	①	1	-0.98146	5.64E+07	122.93
		②	1	-0.98614	1.95E-01	*34.26*
	K$_{A8}$	①	1	-0.97225	1.47E+08	127.56
		②	1	-0.97432	3.36E-01	37.04
20%O$_2$/80%CO$_2$	R$_0$	①	1	-0.97855	1.79E+07	117.21
		②	1	-0.99005	2.06E+02	74.72
	A$_0$	①	1	-0.99368	5.54E+05	105.13
		②	1	-0.98194	1.57E-02	23.68
	K$_{C1}$	①	1	-0.98001	4.89E+06	115.08

		②	1	-0.98029	1.17E+00	44.76
	K_{C3}	①	1	-0.97906	1.01E+03	111.28
		②	1	-0.98572	6.62E-01	41.18
	K_{C5}	①	1	-0.99109	1.40E+07	119.10
		②	1	-0.98918	1.73E+00	45.34
	K_{C8}	①	1	-0.98132	2.62E+07	121.63
		②	1	-0.99555	8.58E-01	41.36
	K_{B1}	①	1	-0.97585	6.74E+06	116.54
		②	1	-0.97227	1.10E+00	44.04
	K_{B3}	①	1	-0.98259	4.28E+05	100.65
		②	1	-0.98784	3.97E-01	37.66
	K_{B5}	①	1	-0.99462	3.28E+06	107.24
		②	1	-0.99519	6.27E+00	54.11
	K_{B8}	①	1	-0.97978	3.27E+04	86.89
		②	1	-0.99284	5.14E-01	41.51
	K_{A1}	①	1	-0.97718	6.61E+05	104.59
		②	1	-0.97170	3.06E-01	37.53
	K_{A3}	①	1	-0.98172	4.53E+06	112.06
		②	1	-0.98838	8.27E-02	30.58
	K_{A5}	①	1	-0.97118	1.29E+07	116.97
		②	1	-0.98511	7.56E-02	30.28
	K_{A8}	①	1	-0.97179	2.50E+06	109.00
		②	1	-0.95940	2.10E-01	35.58
$5\%O_2/95\%N_2$	A_0	①	1	-0.98734	4.50E+02	71.81
		②	1	-0.98798	1.77E-01	36.28
	K_{C5}	①	1	-0.99791	1.01E+05	95.98
		②	1	-0.99066	2.84E-01	37.10
$30\%O_2/70\%N_2$	A_0	①	1	-0.99451	1.20E+06	107.15
		②	1	-0.97586	6.06E-02	29.27
	K_{C5}	①	1	-0.98376	5.87E+07	124.39
		②	1	-0.97600	5.63E-01	38.17
$5\%O_2/95\%CO_2$	A_0	①	1	-0.99660	1.78E+04	89.88
		②	1	-0.97555	3.96E-02	28.56
	K_{C5}	①	1	-0.98816	3.72E+04	92.25
		②	1	-0.99235	3.40E-01	38.93
$30\%O_2/70\%CO_2$	A_0	①	1	-0.99711	5.56E+04	93.47
		②	1	-0.97989	3.84E-02	27.14
	K_{C5}	①	1	-0.98892	9.29E+04	95.16
		②	1	-0.96574	5.45E-01	39.00

Note: ① represents the devolatilization stage; ② represents the char-oxidation stage.

In order to easily analysis, the two kinds of E in the devolatilization stage (①) and in the char-oxidation stage (②) are labeled as E_1 and E_2, respectively. As a comparative, the lowest E_1 and E_2 from the combustion of straw under the same potassium salt type are used to rank the kinetic parameter. In 20%O_2/80%N_2 atmosphere, for the devolatilization stage, the order of E_1 value is: K_{B8} (93.13 kJ mol^{-1}) < K_{A1} (104.66 kJ mol^{-1}) < K_{C8} (113.79 kJ mol^{-1}) < R_0 (115.51 kJ mol^{-1}) < A_0 (117.64 kJ mol^{-1}), while for the char-oxidation stage, the order of E_2 value is: K_{B8} (23.64 kJ mol^{-1}) < K_{C5} (33.57 kJ mol^{-1}) < K_{A5} (34.26 kJ mol^{-1}) < A_0 (34.88 kJ mol^{-1}) < R_0 (59.47 kJ mol^{-1}). However, in 20%O_2/80%CO_2 atmosphere, for the devolatilization stage, the order of E_1 value is: K_{B8} (86.89 kJ mol^{-1}) < K_{A1} (104.59 kJ mol^{-1}) < A_0 (105.13 kJ mol^{-1}) < K_{C3} (111.28 kJ mol^{-1}) < R_0 (117.21 kJ mol^{-1}), while for the char-oxidation stage, the order of E_2 value is: A_0 (23.68 kJ mol^{-1}) < K_{A5} (30.28 kJ mol^{-1}) < K_{B3} (37.66 kJ mol^{-1}) < K_{C3} (41.18 kJ mol^{-1}) < R_0 (74.72 kJ mol^{-1}). The indication of these data is that the catalytic degree order of obtaining the lowest activation energy in the devolatilization stage is K_2CO_3 > KCl > K_2SO_4 in 20%O_2/80%N_2 atmosphere or in 20%O_2/80%CO_2 atmosphere. This result agrees with the foregoing analysis, while in the char-oxidation stage it is K_2CO_3 > K_2SO_4 > KCl in 20%O_2/80%N_2 atmosphere and KCl > K_2CO_3 > K_2SO_4 in 20%O_2/80%CO_2 atmosphere. This is different from the above results due to different loading concentrations and combustion atmospheres. So, it is found that loading potassium salt could decrease the activation energy of the straw combustion in 20%O_2/80%N_2 atmosphere or in 20%O_2/80%CO_2 atmosphere. Also, different potassium salt types, loading concentrations and combustion atmospheres have the different influences on the devolatilization and char-oxidation stages. Overall, the activation energies are generally in accordance with results previously discussed for several samples, considering that the oxy-combustion are unfavorable for chemical reactions due to higher minima in 20%O_2/80%CO_2 atmosphere.

From Table 5, the activation energies for A_0 and K_{C5} under 5%O_2-30%O_2 with N_2 atmospheres are 71.81-117.61 kJ mol^{-1} for E_1 and 29.27-36.28 kJ mol^{-1} for E_2, respectively, while the ones for K_{C5} are 95.98-138.54 kJ mol^{-1} for E_1 and

33.57-38.17 kJ mol^{-1} for E_2, respectively. In addition, in the oxy-biomass combustion atmospheres, the activation energies for A_0 and K_{C5} under 5%O_2-30%O_2 with CO_2 atmospheres are 71.81-117.61 kJ·mol^{-1} for E_1 and 29.27-36.28 kJ mol^{-1} for E_2, respectively, while the ones for K_{C5} are 95.98-138.54 kJ mol^{-1} for E_1 and 33.57-38.17 kJ mol^{-1} for E_2, respectively. These values represent the average activation energies in the devolatilization stage (①) and in the char-oxidation stage (②) during biomass combustion. From these data, it can be concluded that K_{C5} is unfavourable for water washed biomass combustion both in 5%O_2-30%O_2 with N_2 atmospheres and 5%O_2-30%O_2 with CO_2 atmospheres, considering that K_{C5} generally increases the activation energies of combustion and disfavor chemical reactions. This is due to the difference of loading concentration of K_2SO_4. From Table 5, the increase or decrease of the activation energy in the devolatilization stage (E_1) and in the char-oxidation stage (E_2) should be changed as loading concentrations of K_2SO_4. Therefore, water washed biomass loading 5wt.% K_2SO_4 is more difficulty to be degraded than raw water washed biomass.

4. Conclusions

In this paper, the catalysis of potassium on oxy-biomass combustion was studied in a TGA reactor. The effects of potassium salt types (KCl, K_2CO_3, and K_2SO_4), loading concentrations, replacing N_2 by CO_2, and O_2 concentrations on the catalysis degree are discussed. The main conclusions are as follows:

(1) The comparison between TG-DTG curves of straw combustion before and after water washing, in both 20%O_2/80%N_2 and 20%O_2/80%CO_2 atmospheres shows that the water-soluble minerals in biomass play a role in promoting devolatilization and accelerating the biomass char-oxidation; and the replacing of N_2 by CO_2 inhibits both the devolatilization and the char-oxidation processes during oxy-biomass combustion.

(2) In the biomass devolatilization stage, the potassium catalysis degree monotonously increases with the increase of potassium salt loaded concentration. The catalysis degree order of the studied potassium salts is K_2CO_3 > KCl > K_2SO_4. In the char-oxidation stage, with the increase of loading concentration, the three kinds of potassium salts present

inconsistent change tendencies of catalysis degree. In the studied loading concentrations from 0 to 8 wt.%, there is an optimal loading concentration temperatures for KCl and K_2CO_3, at 3 wt.% and 5 wt.%, respectively; while for K_2SO_4, the catalysis degree monotonically increases with the potassium loaded concentration.

(3) For most studied conditions, regardless of the potassium salt types or the loading concentrations or the combustion stages, the catalysis degree in the O_2/CO_2 atmosphere is stronger than that in the O_2/N_2 atmosphere. The catalysis degree is affected by the O_2 concentrations, and the lowest catalysis degree is around 20 vol.% O_2 concentration.

(4) The catalytic degree order of obtaining the lowest activation energy in the devolatilization stage is $K_2CO_3 >$ KCl > K_2SO_4 in 20%O_2/80%N_2 atmosphere or in 20%O_2/80%CO_2 atmosphere, while in the char-oxidation stage it is $K_2CO_3 > K_2SO_4 >$ KCl in 20%O_2/80%N_2 atmosphere and KCl $> K_2CO_3 > K_2SO_4$ in 20%O_2/80%CO_2 atmosphere. Different potassium salt types, loading concentrations and combustion atmospheres have the different influences on the devolatilization and char-oxidation stages.

References

An, H., McGinn, P.J., 2006. Catalytic behavior of potassium containing compounds for diesel soot combustion. Appl. Catal. B-Environ 62 (1-2), 46-56. https://doi.org/10.1016/j.apcatb.2005.06.013.

Backreedy, R.I., Jones, J.M., Pourkashanian, M., Williams, A., 2003. Burn-out of pulverised coal and biomass chars. Fuel 82 (15-17), 2097-2105. https://doi.org/10.1016/S0016-2361(03)00174-1.

Bejarano, P.A., Levendis, Y.A., 2008. Single-coal-particle combustion in O_2/N_2 and O_2/CO_2 environments. Combust.

Flame 153 (1), 270-287. https://doi.org/10.1016/j.combustflame.2007.10.022.

Buhre, B.J.P, Elliott, L.K., Sheng, C.D., Gupta, R.P., Wall, T.F., 2005. Oxy-fuel combustion technology for coal-fired

power generation. Prog. Energ. Combust. 31 (4), 283-307. https://doi.org/10.1016/j.pecs.2005.07.001.

Cerfontain, M.B., Moulijn, J.A., 1983. Alkali-catalysed gasification reactions studied by in situ FTIR spectroscopy. Fuel

62 (2), 256-258. https://doi.org/10.1016/0016-2361(83)90212-0.

Chen, L., Yong, S.Z., Ghoniem, A.F., 2012. Oxy-fuel combustion of pulverized coal: characterization, fundamentals,

stabilization and CFD modeling. Prog. Energ. Combust. 38 (2), 156-214.

https://doi.org/10.1016/j.pecs.2011.09.003.

Coats, A.W., Redfern, J.P., 1964. Kinetic parameters from thermogravimetric data. Nature 201 (4914), 68.

https://doi.org/10.1038/201068a0.

Demirbas, M.F., Balat, M., Balat, H., 2009. Potential contribution of biomass to the sustainable energy development.

Energ. Convers. Manage. 50 (7), 1746-1760. https://doi.org/10.1016/j.enconman.2009.03.013.

Deng, L., Zhang, T., T., Che, D., 2013. Effect of water washing on fuel properties, pyrolysis and combustion

characteristics, and ash fusibility of biomass. Fuel Process. Technol. 106, 712-720.

https://doi.org/10.1016/j.fuproc.2012.10.006.

Fang, M.X., Shen, D.K., Li, Y.X., Yu, C.J., Luo, Z.Y., Cen, K.F., 2006. Kinetic study on pyrolysis and combustion of

wood under different oxygen concentrations by using TG-FTIR analysis. J. Anal. Appl. Pyrol, 77 (1), 22-27.

https://doi.org/10.1016/j.jaap.2005.12.010.

Freriks, I.L.C., Van Wechem, H.M.H., Stuiver, J.C.M., Bouwman, R., 1981. Potassium-catalysed gasification of carbon

with steam: a temperature-programmed desorption and Fourier Transform infrared study. Fuel 60 (6), 463-470.

https://doi.org/10.1016/0016-2361(81)90104-6.

Gil, M.V., Riaza, J., Álvarez, L., Pevida, C., Pis, J.J., Rubiera, F., 2012. Oxy-fuel combustion kinetics and morphology

of coal chars obtained in N_2 and CO_2 atmospheres in an entrained flow reactor. Appl. Energ. 91 (1), 67-74. https://doi.org/10.1016/j.apenergy.2011.09.017.

Gómez-Barea, A., Ollero, P., 2006. An approximate method for solving gas–solid non-catalytic reactions. Chem. Eng. Sci 61 (11), 3725-3735. https://doi.org/10.1016/j.ces.2005.12.023.

Jayaraman, K., Gökalp, I., 2015. Pyrolysis, combustion and gasification characteristics of miscanthus and sewage sludge. Energ. Convers. Manage. 89, 83-91. https://doi.org/10.1016/j.enconman.2014.09.058.

Jensen, A., Dam-Johansen, K., Wójtowicz, M.A., Serio, M.A., 1998. TG-FTIR study of the influence of potassium chloride on wheat straw pyrolysis. Energ. Fuel. 12 (5), 929-938. https://doi.org/10.1021/ef980008i.

Jones, J.M., Darvell, L.I., Bridgeman, T.G., Pourkashanian, M., Williams, A., 2007. An investigation of the thermal and catalytic behaviour of potassium in biomass combustion. P. Combust. Inst. 31(2), 1955-1963. https://doi.org/10.1016/j.proci.2006.07.093.

Li, S., Wei, X., 2013. Numerical Simulation of CO and NO Emissions During Converter Off-Gas Combustion in the Cooling Stack. Combust. Sci. Technol. 185(2), 212-225. https://doi.org/10.1080/00102202.2012.715606.

Ma, X., Li, Y., Shi, L., He, Z., Wang, Z., 2016. Fabrication and CO_2 capture performance of magnesia-stabilized carbide slag by by-product of biodiesel during calcium looping process. Appl. Energ. 168, 85-95. https://doi.org/10.1016/j.apenergy.2016.01.080.

McKee, D.W., 1983. Mechanisms of the alkali metal catalysed gasification of carbon. Fuel 62 (2), 170-175. https://doi.org/10.1016/0016-2361(83)90192-8.

Nowakowski, D.J., Jones, J.M., Brydson, R.M., Ross, A.B., 2007. Potassium catalysis in the pyrolysis behaviour of short rotation willow coppice. Fuel 86(15), 2389-2402. https://doi.org/10.1016/j.fuel.2007.01.026.

Nzihou, A., Stanmore, B., Sharrock, P., 2013. A review of catalysts for the gasification of biomass char, with some reference to coal. Energy 58, 305-317. https://doi.org/10.1016/j.energy.2013.05.057.

Querini, C.A., Cornaglia, L.M., Ulla, M.A., Miro, E.E., 1999. Catalytic combustion of diesel soot on Co, K/MgO catalysts. Effect of the potassium loading on activity and stability. Appl. Catal. B-Environ 20 (3), 165-177. https://doi.org/10.1016/S0926-3373(98)00109-X..

Quyn, D.M., Wu, H., li, C.Z., 2002. Volatilisation and catalytic effects of alkali and alkaline earth metallic species during the pyrolysis and gasification of Victorian brown coal. Part I. Volatilisation of Na and Cl from a set of NaCl-loaded samples. Fuel 81 (2), 143-149. https://doi.org/10.1016/S0016-2361(01)00127-2.

Ren, Q., Li, L., 2015. Co-combustion of Agricultural Straw with Municipal Sewage Sludge in a Fluidized Bed: Role of Phosphorus in Potassium Behavior. Energ. Fuel. 29 (7), 4321-4327. https://doi.org/10.1021/acs.energyfuels.5b00790.

Shen, B., Qin, L., 2006. Study on MSW catalytic combustion by TGA. Energ. Convers. Manage. 47 (11), 1429-1437. https://doi.org/10.1016/j.enconman.2005.08.016.

Sima-Ella, E., Mays, T.J., 2005. Analysis of the oxidation reactivity of carbonaceous materials using thermogravimetric analysis. J. Therm. Anal. Calorim. 80 (1), 109-113. https://doi.org/10.1007/s10973-005-0621-x.

Su, W., Ma, H., Wang, Q., Li, J., Ma, J., 2013. Thermal behavior and gaseous emission analysis during co-combustion of ethanol fermentation residue from food waste and coal using TG–FTIR. J. Anal. Appl. Pyrol 99, 79-84. https://doi.org/10.1016/j.jaap.2012.10.023.

Toftegaard, M.B., Brix, J., Jensen, P.A., Glarborg, P., Jensen, A.D., 2010. Oxy-fuel combustion of solid fuels. Prog. Energ. Combust. 36 (5), 581-625. https://doi.org/10.1016/j.pecs.2010.02.001.

Wagner, R., Mühlen, H.J., 1989. Effect of a catalyst on combustion of char and anthracite. Fuel 68 (2), 251-253. https://doi.org/10.1016/0016-2361(89)90333-5.

Wang, L., Skjevrak, G., Hustad, J.E., Skreiberg, Ø., 2013. Investigation of biomass ash sintering characteristics and the effect of additives. Energ. Fuel. 28 (1), 208-218. https://doi.org/10.1021/ef401521c.

Wang, X., Hu, Z., Deng, S., Wang, Y., Tan, H, 2015a. Kinetics investigation on the combustion of biochar in O_2/CO_2

atmosphere. Environ. Prog. Sustain. 34 (3), 923-932. https://dx.doi.org/10.1002/ep.12063.

Wang, X., Hu, Z., Deng, S., Wang, Y., Wei, B., Tan, H., 2014. Investigation on the synergetic effect of biomass co-firing

in the atmosphere of O_2/CO_2. J. Biobased Mater. Bio. 8 (5), 481-488. https://doi.org/10.1166/jbmb.2014.1460.

Wang, X., Li, S., Adeosun, A., Li, Y., Vujanović, M., Tan, H., Duić, N., 2017. Effect of potassium-doping and oxygen

concentration on soot oxidation in O_2/CO_2 atmosphere: A kinetics study by thermogravimetric analysis. Energ.

Convers. Manage. 149, 686-697. https://www.sciencedirect.com/science/article/pii/S0196890417300031.

Wang, X., Liu, Y., Tan, H., Ma, L., Xu, T., 2012. Mechanism research on the development of ash deposits on the heating

surface of biomass furnaces. Ind. Eng. Chem. Res. 51 (39), 12984-12992. https://doi.org/10.1021/ie302009m.

Wang, X., Tan, H., Niu, Y., Pourkashanian, M., Ma, L., Chen, E., Liu, Y., Liu, Z., Xu, T.. 2011. Experimental

investigation on biomass co-firing in a 300MW pulverized coal-fired utility furnace in China. P. Combust. Inst. 33

(2), 2725-2733. https://doi.org/10.1016/j.proci.2010.06.055.

Wang, Y., Wang, X., Tan, H., Du, W., Qu, X., 2015b. Extraction and quantitation of various potassium salts in straw ash.

Environ. Prog. Sustain. 34 (2), 333-338. https://dx.doi.org/ 10.1002/ep.11988.

Zhou, Y., Jin, X., Jin, Q., 2016. Numerical investigation on separate physicochemical effects of carbon dioxide on coal

char combustion in O_2/CO_2 environments. Combust. Flame 167, 52-59.

https://doi.org/10.1016/j.combustflame.2016.02.028.